Solid State Ionics 291 (2016) 1–7

Contents lists available at ScienceDirect

Solid State Ionics

journal homepage: www.elsevier.com/locate/ssi

Mechanism of lithium ion diffusion in the hexad substituted $Li_7La_3Zr_2O_{12}$ solid electrolytes

Y.X. Gao, X.P. Wang *, H. Lu, L.C. Zhang, L. Ma, Q.F. Fang *

Key Laboratory of Materials Physics, Institute of Solid State Physics, Chinese Academy of Sciences, Hefei 230031, People's Republic of China

ARTICLE INFO

Article history:
Received 12 January 2016
Accepted 22 April 2016
Available online 2 May 2016

Keywords:
Garnet-type oxides
Li–La–M–O system
Lithium ions diffusion
Internal friction

ABSTRACT

The $Li_{6.4}La_3Zr_{1.7}M_{0.3}O_{12}$ (M = Mo and Cr) and $Li_{7-2x}La_3Zr_{2-x}W_xO_{12}$ ($x = 0.1$–0.5) solid lithium-ion conductors were prepared by conventional solid state reaction method. The results indicate that partial substitutions by W and Mo ions can stabilize the garnet-like cubic phase of Li–La–Zr–O at room temperature, while the Cr ions substitution cannot even at a content of 15 mol%. The total conductivity of the $Li_{7-2x}La_3Zr_{2-x}W_xO_{12}$ lithium conductor is the highest at $x = 0.2$ (8.7×10^{-5} S/cm), and decreases with the increasing W substituting concentration. The $Li_{6.4}La_3Zr_{1.7}Mo_{0.3}O_{12}$ has a higher total conductivity than that of $Li_{6.4}La_3Zr_{1.7}W_{0.3}O_{12}$. Different from one apparent peak in the $Li_7La_3Zr_2O_{12}$ samples, two prominent relaxation-type internal friction peaks related to the short range diffusion of lithium ions were observed in each W or Mo substituted $Li_7La_3Zr_2O_{12}$ compounds. The high-temperature IF peaks locate at about 365.9 K and 358.9 K at 1 Hz, corresponding to an activation energy of 0.49 and 0.51 eV for the W and Mo substituted $Li_7La_3Zr_2O_{12}$ compounds, respectively. Considering the crystalline structure, it was suggested that the lithium ionic diffusion between 48g(96h)-24d corresponds to the low-temperature peak and 48g(96h)-48g(96h) to the high-temperature peak.

1. Introduction

The large-scale applications of rechargeable lithium ion batteries for electronics and power sources need high safety electrolyte materials with high lithium ion conductivity. Comparing with liquid organic-polymer electrolytes, solid electrolyte materials can well satisfy the requirements of high safety. Furthermore, the solid electrolytes generally exhibit more advantages, such as high mechanical performance, and low toxicity. However, the lower lithium ionic conductivity or electrochemical stability limits their actual application in rechargeable lithium batteries [1–4].

The Li ion conducting garnet-type oxides Li–La–M–O (M = Nb, Ta, Bi, Zr) have been considered as one kind of promising electrolytes because of their high conductivity and stability with metallic lithium [5–8]. Especially the so-called stuffed lithium garnet $Li_7La_3Zr_2O_{12}$ has attracted much attention due to its relatively high ionic conductivity (3×10^{-4} S/cm at 25 °C, which is now approaching that of organic electrolytes [9]) but negligible electronic conductivity as a solid electrolyte for lithium batteries.

The $Li_7La_3Zr_2O_{12}$ compound exhibits two different phase structures: tetragonal (space group I41/acd) and cubic (space group $Ia\bar{3}d$) phases [10]. For the tetragonal $Li_7La_3Zr_2O_{12}$, the lithium ions distribute in an ordered state, and all Li sites with the same symmetry are either fully occupied or completely empty, which leads to a poor lithium ionic conductivity. However in the cubic phase, lithium ions distribute in a disordered state and the Li sites with the same symmetry are only partially occupied. The partial accommodation and disordered distribution of lithium ions result in the high conductivity [11]. It has been proven that the conductivity of the tetragonal phase is two orders of magnitude lower than that of the cubic phase [12]. Hence it is a key issue how to prepare the cubic phase $Li_7La_3Zr_2O_{12}$.

So far, there are two ways to effectively prepare the $Li_7La_3Zr_2O_{12}$ based cubic phase. One is the long time sintering at temperatures of 1200 °C or above, which has also been thought to be the key factor controlling the transformation from tetragonal to cubic [9]. The other is the partial cationic substitution. Recent studies showed that the existence of cubic structure at room temperature is attributed to the substituting by cations such as aluminum [9,13,14], yttrium [15] or tantalum [16] ions. For example, it is suggested that a possible chemical reaction between the molten precursors (Li_2CO_3 or LiOH) and the crucible wall during the heat treatment results in the introduction of Al ions into the garnet crystal and stabilizes the cubic phase at room temperature [9]. In addition, doping aluminum [17] or tantalum [16] could induce the formation of the stable cubic LLZ at 1000 °C or 1120 °C, respectively, which is helpful for preparing the bulk ceramic with a higher density at a lower temperature. Therefore, for the cubic phase formation and conductivity enhancement it is necessary to explore the suitable substituting element and its optimum substitution concentration.

In view of the conducting essence in solid state lithium electrolytes, as the ionic conductivity in the lithium electrolytes mainly depends on the migrations of lithium ions via vacancies, it is necessary to gain a

* Corresponding authors.
E-mail addresses: xpwang@issp.ac.cn (X.P. Wang), qffang@issp.ac.cn (Q.F. Fang).

http://dx.doi.org/10.1016/j.ssi.2016.04.017
0167-2738/

fundamental understanding of the key factors that control fast ion diffusion. So far, although a number of studies have been carried out to investigate the crystal structure and conductivity of the garnet-type lithium electrolytes based on experimental investigation and theoretical simulation, the underlying mechanism of lithium ion migration is still controversial. The internal friction (designated as IF) is a measure of the ability of materials to dissipate mechanical energy. As a technique sensitive to the ion migration, this method has been successfully employed to investigate the transport properties of oxygen ions [18] and lithium ions [19,20]. Different from the electrochemical impedance spectroscopy, the IF method can distinguish different short range migration processes of point defects in detail, because different migration processes of defects will be related to different characteristic IF peaks, which correspond to different peak positions, peak shapes as well as relaxation parameters.

Cr, Mo and W are group VIB elements with hexads. Substitution of each M^{6+} for Zr^{4+} in $Li_{7-2x}La_3Zr_{2-x}M_xO_{12}$ electrolytes can result in two more intrinsic lithium vacancies, and thus adjust the lithium conductivity of the $Li_7La_3Zr_2O_{12}$ electrolytes. In another side, Cr, Mo and W with different ionic radius may lead to a change in lattice constant of $Li_7La_3Zr_2O_{12}$ electrolytes which also has a large impact on the lithium conductivity. So in this paper the IF method combining with AC impedance spectroscopy was employed to investigate the effect of partial substitution of W, Cr and Mo elements on the cubic phase stabilization and lithium ionic conductivity and the detailed lithium ionic diffusion mechanism in cubic phase Li–La–Zr–O based garnet like electrolytes.

2. Experimental details

Polycrystalline powders of $Li_{6.4}La_3Zr_{1.7}M_{0.3}O_{12}$ (M = Mo and Cr) and $Li_{7-2x}La_3Zr_{2-x}W_xO_{12}$ ($x = 0.1$–0.5) were synthesized by the solid state reaction method. A mixture of Li_2CO_3 (99.99%), La_2O_3 (99.99%), ZrO_2 (99.99%), WO_3 (99.995%), CrO_3 (99.9%) or MoO_3 (99.9%) in the above mentioned ratio was prepared as the precursors. The detailed synthesis processes have been reported in our previous work [21].

The phase composition of all the investigated M-substituted $Li_7La_3Zr_2O_{12}$ oxides was characterized with X-ray diffraction (XRD) patterns by using Cu-Kα radiations at room temperature in a scanning range from 10° to 70° with a step of 0.033°. Structural refinement was done using the Fullprof suite of Rietveld software [22], in which the pseudo-Voigt function was used as the profile function.

The lithium ionic conductivity of the M-substituted $Li_7La_3Zr_2O_{12}$ pellets at different temperatures was measured using a computer-controlled frequency response analyzer (Hioki 3531 Z-Hitester) in the frequency range from 42 Hz to 5 MHz at a voltage amplitude of 0.05 V. Silver paste served as electrode was painted on both side of the wafer-shaped samples and sintered at 873 K for 1 h. All samples were stabilized at a measured temperature for at least 30 min at the beginning of the impedance measurement.

The measurements of low frequency internal friction (IF) were carried out on a computer controlled inverted torsion pendulum in the forced vibration mode with a heating rate of 1 K/min, and the measurement frequencies were chosen as 0.5 Hz, 1 Hz, 2 Hz and 4 Hz, respectively. The maximum torsion strain amplitude was kept at 1.5×10^{-5} in all the measurements. The size of the strip samples is about 50 mm × 4 mm × 1 mm.

3. Results and discussion

3.1. XRD analysis

Fig. 1(a) shows the measured powder XRD patterns for the $Li_{6.4}La_3Zr_{1.7}M_{0.3}O_{12}$ (M = Cr, Mo and W) ceramics sintered at 1373 K for 9 h. It can be seen that the powder XRD patterns of samples substituted with W and Mo exhibit the pure cubic garnet like structures without any impurity phases. The study reveals that the substitution of

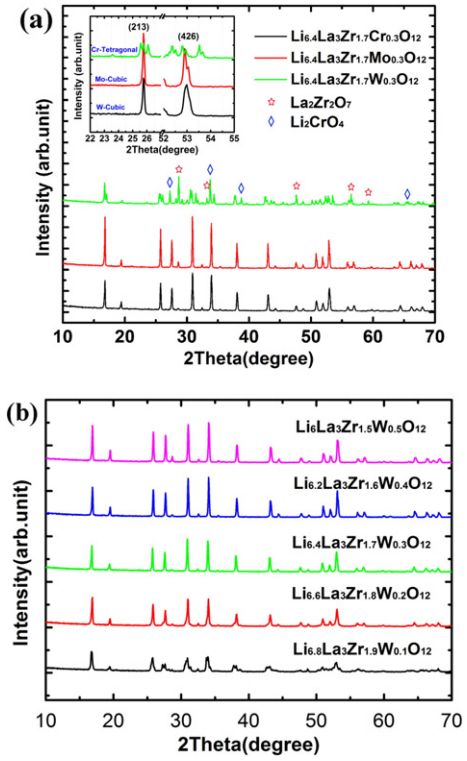

Fig. 1. (a) Powder XRD patterns of $Li_{6.4}La_3Zr_{1.7}M_{0.3}O_{12}$ (M = W, Cr, Mo) ceramics sintered at 1373 K for 9 h. Inset in (a): the enlarged diffraction (213) and (426) lines. (b) The powder XRD patterns of $Li_{7-2x}La_3Zr_{2-x}W_xO_{12}$ ($x = 0.1$–0.5) ceramics sintered at 1373 K for 9 h.

Zr by 15 mol% W or Mo can completely stabilize the Li–La–Zr–O garnet-like cubic phase. However, a significant tetragonal splitting is observed in the $Li_{6.4}La_3Zr_{1.7}Cr_{0.3}O_{12}$, as evidenced by the enlarged local (213) and (426) diffraction lines in the inset [11]. In addition, the XRD pattern of Cr substituted sample exhibits additional reflection corresponding to impurity phase of $La_2Zr_2O_7$ (JCPDS: 17-0450) and Li_2CrO_4 (JCPDS: 31-0715). This illustrates that Cr substituting is not an effective way to stabilize the cubic phase of Li–La–Zr–O garnet-like ceramics because its ionic radius (0.044 nm, VI coordination) is too small in comparison with that of Zr ions (0.072 nm). Therefore, the following investigations will not cover the Cr substituted samples.

To investigate the effect of substitution content, $Li_{7-2x}La_3Zr_{2-x}W_xO_{12}$ ($x = 0.1$–0.5) samples were prepared. Fig. 1(b) shows the XRD patterns of $Li_{7-2x}La_3Zr_{2-x}W_xO_{12}$ ($x = 0.1$–0.5) ceramics powders sintered at 1373 K for 9 h. It can be seen that the main diffraction peaks of the $Li_{7-2x}La_3Zr_{2-x}W_xO_{12}$ with $x = 0.1$ exhibit tetragonal phase and additional weak reflections correspond to minor impurity phase of $La_2Zr_2O_7$ (JCPDS: 17-0450) and La_2O_3 (JCPDS: 22-0369). When the W substituting concentration reaches $x = 0.2$ or higher, only pure garnet-type cubic phases are detected and no other impurity phases are found in the XRD patterns. This implies that the W substitution at Zr sites with concentration of 10 mol% ($x = 0.2$) or higher can stabilize the cubic phase of Li–La–Zr–O garnet-like ceramics at room temperature.

The single garnet-like phases $Li_{6.4}La_3Zr_{1.7}Mo_{0.3}O_{12}$ and $Li_{7-2x}La_3Zr_{2-x}W_xO_{12}$ ($x = 0.2$–0.5) can be all well indexed by space group $Ia\bar{3}d$, and the fitting result of $Li_{6.4}La_3Zr_{1.7}W_{0.3}O_{12}$ is shown for example in Fig. 2. The cell parameters of the W and Mo substituted samples with $x = 0.3$ are determined from the refinement, which are about 12.93(3) Å and 12.94(9) Å, respectively. The cell parameter of the W substituted samples is in agreement with the value reported in reference [23].

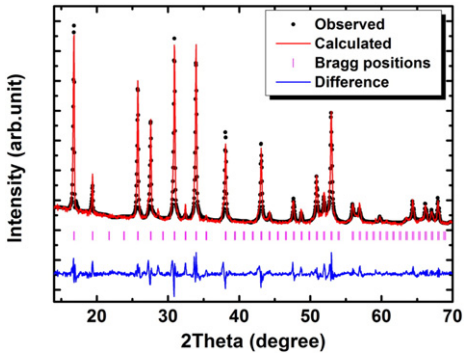

Fig. 2. The observed, calculated, Bragg positions and deference of the Rietveld refinement from the X-ray diffraction patterns of cubic $Li_{6.4}La_3Zr_{1.7}W_{0.3}O_{12}$ using a space group $Ia\bar{3}d$.

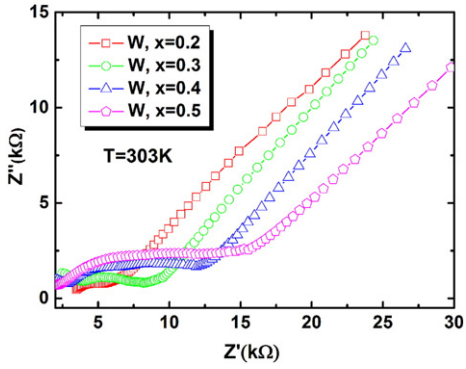

Fig. 4. Impedance spectra of $Li_{7-2x}La_3Zr_{2-x}W_xO_{12}$ ($x = 0.2$–0.5) pellets measured at room temperature.

Fig. 3 shows the variation of lattice parameters of the $Li_{7-2x}La_3Zr_{2-x}W_xO_{12}$ with W concentrations. It is found that the cell parameter decreases linearly with the increasing W content, which obeys the so-called Vegard's law. The substitution of smaller W^{6+} (ionic radius ~0.060 nm) for the larger Zr^{4+} (~0.072 nm) under the same six-coordinate environments leads to decrease of the lattice constant [24]. In addition, the cell parameter of Mo sample is also smaller than that of $Li_7La_3Zr_2O_{12}$ sample, which is also attributed to the smaller ionic radius of Mo (~0.059 nm, VI coordination).

3.2. Ionic conductivity

The lithium ionic conductivity of the $Li_{7-2x}La_3Zr_{2-x}M_xO_{12}$ (M = Mo, $x = 0.3$ and W, $x = 0.2$–0.5) ceramics is determined by AC impedance spectroscopy. The complex impedance spectra of $Li_{7-2x}La_3Zr_{2-x}W_xO_{12}$ ($x = 0.2$–0.5) pellets at room temperatures and $Li_{6.4}La_3Zr_{1.7}Mo_{0.3}O_{12}$ at 303 K and 323 K are presented in Figs. 4 and 5, respectively. As well known, the impedance spectrum of the bulk materials usually shows three semicircles or two semicircles in high-frequency and a low-frequency tail, which correspond to the bulk resistance, grain boundary or interface resistance, and electrode reaction impedance, respectively. However, in the present case not every impedance spectrum has the two depressed semicircles observed on the high frequency side in the Nyquist spectrum, such as $Li_{6.6}La_3Zr_{1.8}W_{0.2}O_{12}$ and $Li_{6.4}La_3Zr_{1.7}Mo_{0.3}O_{12}$. The observed impedance spectra for grain resistance and grain boundary resistance overlapped with each other and cannot be obviously separated from the impedance plots. Hence the total sum of the bulk and grain-boundary contributions is therefore used to evaluate the conduction properties of $Li_{7-2x}La_3Zr_{2-x}M_xO_{12}$ (M = Mo, $x = 0.3$ and W, $x = 0.2$–0.5) in our case, similar to the case of other garnet-like Li–La–M–O (M = Bi, Ta, Zr) lithium conductors [6,11,25]. At the lower frequency range, a typical polarized tail is observed in each AC spectroscopy, indicating that the investigated garnet-like $Li_{7-2x}La_3Zr_{2-x}W_xO_{12}$($x = 0.2$–$0.5$) and $Li_{6.4}La_3Zr_{1.7}Mo_{0.3}O_{12}$ compounds are actually ionic conductors [26]. The total lithium ionic conductivity can be determined according to the equation $\sigma_t = L / (SR_t)$ (where L and S are the thickness and area of the sample, respectively, and R_t is the total resistance including the bulk and grain boundary resistance). The corresponding results are listed in Table 1.

The temperature dependence of the total conductivity of $Li_{7-2x}La_3Zr_{2-x}W_xO_{12}$ ($x = 0.2$–0.5) and $Li_{6.4}La_3Zr_{1.7}Mo_{0.3}O_{12}$ samples was shown in Fig. 6. According to the Arrhenius relation: $\sigma T = A\exp(-E / kT)$ (where A is the pre-exponential factor, E is the activation energy and T is the absolute temperature), the activation energy E for lithium ionic transport in the $Li_{7-2x}La_3Zr_{2-x}W_xO_{12}$ ($x = 0.2$–0.5) and $Li_{6.4}La_3Zr_{1.7}Mo_{0.3}O_{12}$ samples can be determined. The activation energies are in the range of 0.45–0.49 eV and listed in Table 1. The obtained activation energy data are typical for lithium ion diffusion in cubic garnet-type lithium electrolytes and comparable to the reported value of 0.45 eV [23].

From the experimental results it can be seen that the total conductivity of the $Li_{7-2x}La_3Zr_{2-x}W_xO_{12}$ lithium conductors exhibits the highest value at $x = 0.2$ (8.7×10^{-5} S/cm), and decreases with the increasing W substituting concentration in the range of x = 0.2–0.5. It is well known that the lithium ionic conductivity depends mainly on the mobile lithium ions concentration (denoted by n) and the mobility of the lithium ions (denoted by D). According to the principle of charge compensation, each M^{6+} substitution for Zr^{4+} in $Li_{7-2x}La_3Zr_{2-x}M_xO_{12}$ electrolytes can result in the decrease of two lithium ions to maintain electrical neutrality. With the increasing W substituting concentration, the value of n decreases gradually, which may lead to the decrease of total lithium ionic conductivity. And again, the lattice constant evidenced by the XRD results decreases gradually with the increasing W substituting concentration, and the narrower lithium ions migration channels caused by larger lattice distortion is unfavorable for lithium migration in lattice. These points finally lead to the decrease of the

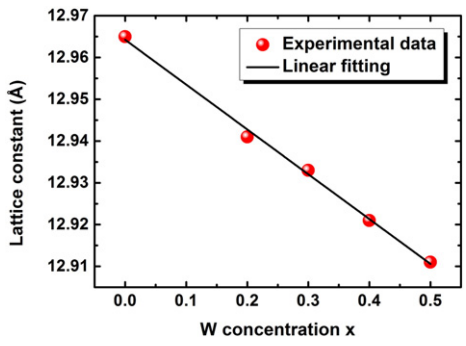

Fig. 3. Evolution of cell parameter with W concentration x for $Li_{7-2x}La_3Zr_{2-x}W_xO_{12}$.

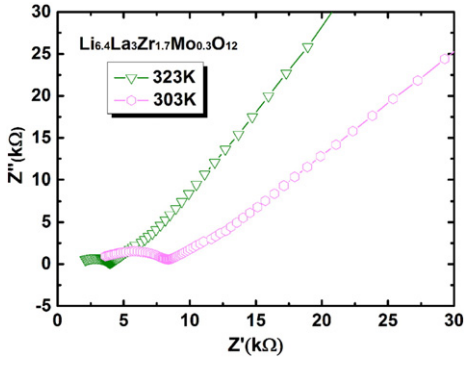

Fig. 5. Impedance spectra of $Li_{6.4}La_3Zr_{1.7}Mo_{0.3}O_{12}$ pellet measured at 303 K and 323 K.

Table 1
The total lithium ionic conductibility and activation energy of $Li_{7-2x}La_3Zr_{2-x}W_xO_{12}$ ($x = 0.2$–0.5) and $Li_{6.4}La_3Zr_{1.7}Mo_{0.3}O_{12}$ samples.

$Li_{7-x}La_3Zr_{2-x}M_xO_{12}$	M = W				M = Mo
	$x = 0.2$	$x = 0.3$	$x = 0.4$	$x = 0.5$	$x = 0.3$
E(eV) (±0.02 eV)	0.45	0.46	0.48	0.49	0.45
σ(S/cm) ($\pm 0.1 \times 10^{-5}$ S/cm)	8.7×10^{-5}	5.8×10^{-5}	4.2×10^{-5}	3.5×10^{-5}	7.6×10^{-5}

lithium ions mobility, and as a result M^{6+} partial substitution for Zr^{4+} in $Li_{7-2x}La_3Zr_{2-x}M_xO_{12}$ electrolytes result in a larger activation energy which increases from 0.45 eV to 0.49 eV with the increasing W substituting concentration. The mobility of the lithium ions may be the more important factor leading to a decreased lithium ionic conductivity for $Li_{7-2x}La_3Zr_{2-x}W_xO_{12}$ (x = 0.2–0.5) samples comparing with the influence of lithium ions concentration *n*. The similar situation has been reported in Ref. [27].

The total conductivity of $Li_{6.4}La_3Zr_{1.7}Mo_{0.3}O_{12}$ samples is about 7.6×10^{-5} S/cm at 303 K and 1.8×10^{-4} S/cm at 323 K. Comparing with the value of W substituted sample (5.8×10^{-5} S/cm at 303 K and 1.4×10^{-4} S/cm at 323 K, respectively) with the same substituting level of 0.3, the $Li_{6.4}La_3Zr_{1.7}Mo_{0.3}O_{12}$ sample has a higher lithium ionic conductivity. The total conductivity at the same temperature is mainly controlled by the mobility of Li ions. The higher total conductivity of the $Li_{6.4}La_3Zr_{1.7}Mo_{0.3}O_{12}$ sample may be attributed to the lower activation energy of 0.45 eV comparing with the value of 0.46 eV for $Li_{6.4}La_3Zr_{1.7}W_{0.3}O_{12}$ sample. The lower activation energy in the $Li_{6.4}La_3Zr_{1.7}Mo_{0.3}O_{12}$ may be attributed to the larger lattice constant by Mo partial substitution comparing with that of W substituting, which may supply a wide migration pathway for lithium ions diffusion.

3.3. Internal friction (IF)

Fig. 7(a) and (b) present the temperature dependence of the internal friction (IF) (Q^{-1}) and the relative modulus (M) at four different frequencies of 0.5 Hz, 1 Hz, 2 Hz, and 4 Hz for $Li_{6.4}La_3Zr_{1.7}M_{0.3}O_{12}$ (M = W, Mo) samples. Two well developed IF peaks (labeled as P_{WL} and P_{WH} for W substituting sample and P_{ML} and P_{MH} for Mo substituting sample, respectively) are observed in the temperature spectra for each frequency, accompanied by a corresponding decrease of modulus near the peak position. The peak positions all shift obviously toward higher temperature with the increasing measurement frequency, while the peak height or relaxation strength hardly changes with frequency. It demonstrates that these peaks should be associated with a thermally activated relaxation process [28], such as the short-distance jump processes of lithium ions or vacancies.

Fig. 8 shows the IF spectrum of $Li_{7-2x}La_3Zr_{2-x}W_xO_{12}$ ($x = 0.2$–0.5) at 1 Hz. It can be seen that the relaxation strength of the two IF peaks is all closely related to the W concentration and decreases with the increasing W concentration in the range of $x = 0.2$–0.5. According to the theory of point defects relaxation, the relaxation strength of the IF peak is proportional to the concentration of relaxation species and the square of the dipole shape factor based on the concept that each point defect behaves like an elastic dipole [28]. Therefore, from the variation of the relaxation strength of the two prominent relaxation peaks with W substituting content, the $Li_{6.6}La_3Zr_{1.8}W_{0.2}O_{12}$ samples should have higher concentration of relaxation species than the $Li_6La_3Zr_{1.5}W_{0.5}O_{12}$ samples. Fig. 9 shows the IF spectrum of $Li_{6.4}La_3Zr_{1.7}Mo_{0.3}O_{12}$, $Li_{6.4}La_3Zr_{1.7}W_{0.3}O_{12}$ and $Li_7La_3Zr_2O_{12}$ at 1 Hz for comparison. In the $Li_{6.4}La_3Zr_{1.7}W_{0.3}O_{12}$ samples, the two prominent separated IF peaks are located around 290 K and 365 K with a peak height as high as 0.035 and 0.015, respectively. For the $Li_{6.4}La_3Zr_{1.7}Mo_{0.3}O_{12}$ samples however, although the peak positions are similar with that of W-substituted sample, the peak height of the low-temperature peak is about two times that of W-substituted sample but the high-temperature IF peak is lower. However in the $Li_7La_3Zr_2O_{12}$ only one apparent peak with a height of about 0.10 was detected, according to the existence of mutual interaction among lithium ions, the only one IF peak can be decomposed into two closely overlapped peaks as shown in Fig. 9 [11]. By contrast, the IF peaks in the $Li_{7-2x}La_3Zr_{2-x}M_xO_{12}$ (M = Mo and W) were splitted into two well separated IF peaks. Hence on one side, the two apparently separated IF peaks observed in

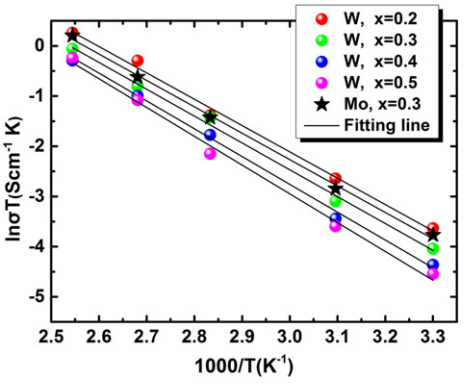

Fig. 6. Temperature dependence of total ionic conductivity of the $Li_{7-2x}La_3Zr_{2-x}W_xO_{12}$ ($x = 0.2$–0.5) and $Li_{6.4}La_3Zr_{1.7}Mo_{0.3}O_{12}$ compounds.

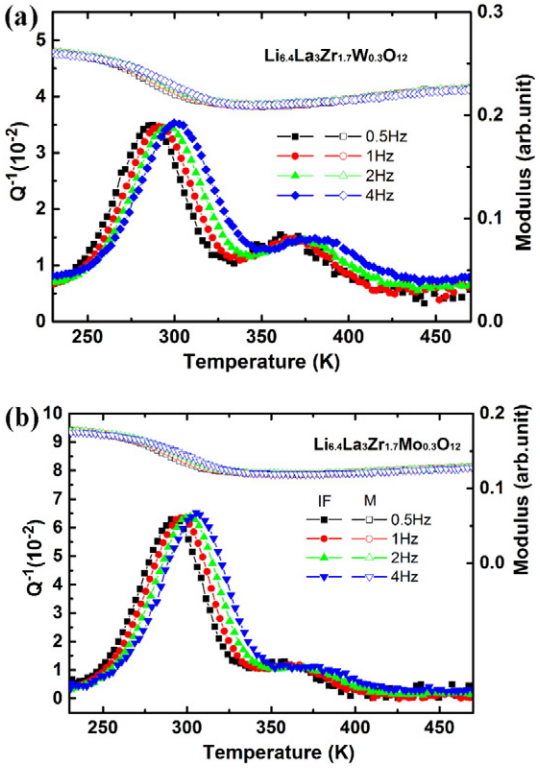

Fig. 7. Temperature dependence of the internal friction (Q^{-1}) and the relative modulus (M) of the $Li_{6.4}La_3Zr_{1.7}W_{0.3}O_{12}$ (a) and $Li_{6.4}La_3Zr_{1.7}Mo_{0.3}O_{12}$ (b) samples measured at four different frequencies (0.5, 1, 2 and 4 Hz) with a heating rate of 2 K/min.

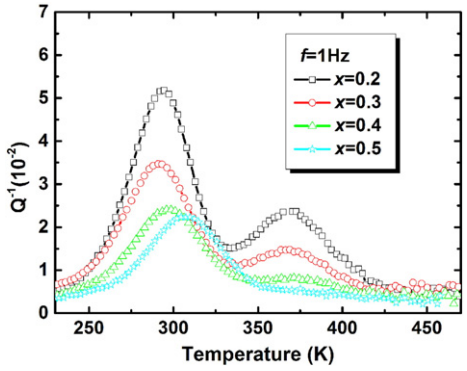

Fig. 8. W substitution concentration dependence of internal friction spectra at 1 Hz in the $Li_{7-2x}La_3Zr_{2-x}W_xO_{12}$ ($x = 0.2$–0.5) samples.

the hexad substituted $Li_7La_3Zr_2O_{12}$ electrolytes demonstrate convincingly the rationality of two sub-peaks assumption in $Li_7La_3Zr_2O_{12}$ samples. On the other side, it means that the peak position of the high-temperature IF peak at 1 Hz shifts to higher temperature of about 365.9 K and 358.9 K for W and Mo substituted $Li_7La_3Zr_2O_{12}$ compounds, respectively. Comparing with that of $Li_7La_3Zr_2O_{12}$ sample, the shift of the peak position is probably due to the larger activation energy and a decreased mobility of the lithium ions as discussed later. In addition, the lattice constant evidenced by the XRD results is about 12.965 Å for $Li_7La_3Zr_2O_{12}$ electrolyte [11], which is much higher than the value of 12.933 Å for $Li_{6.4}La_3Zr_{1.7}W_{0.3}O_{12}$ electrolyte and 12.949 Å for $Li_{6.4}La_3Zr_{1.7}Mo_{0.3}O_{12}$. The larger lattice distortion may be the other reason for the peak position shift of the high-temperature IF peak.

The common theoretical models for relaxation-type peaks are Debye model or coupling model. The Debye model is for the system where the mutual interaction between the relaxation species is small enough to be neglected. However the coupling model is usually for the system with a strong mutual interaction among high concentration lithium ions. In lithium electrolytes, the diffusion processes of lithium ions are not isolated but collaborative in nature because of the strong mutual interaction among high concentration lithium ions. And it is well known that the mutual interaction among high concentration lithium ions can be well described by the coupling model [29,30]. Hence in this paper it is assumed that the two IF peaks in $Li_{7-2x}La_3Zr_{2-x}M_xO_{12}$ (M = Mo and W) can also be fitted by the coupling model. According to this model, the correlation function $C(t)$ can be separated into two regions by a crossover time t_c, that is,

$$C(t) = exp(-t/t^*) \quad \text{for } t<t_c \tag{1}$$

$$C(t) = exp\left[-(t/t)^{\beta}\right] \quad \text{for } t>t_c \tag{2}$$

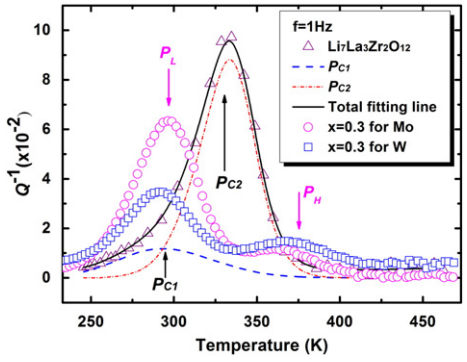

Fig. 9. Internal friction spectra at 1 Hz of the $Li_{6.4}La_3Zr_{1.7}W_{0.3}O_{12}$, $Li_{6.4}La_3Zr_{1.7}Mo_{0.3}O_{12}$ and $Li_7La_3Zr_2O_{12}$ samples.

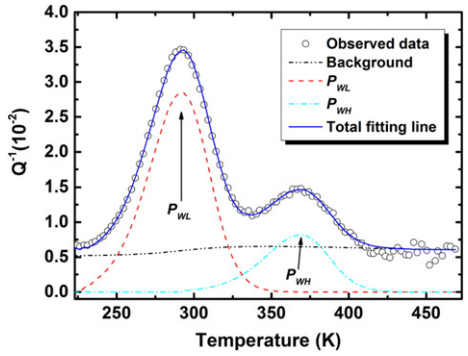

Fig. 10. Fitting results of the internal friction spectrum at 1 Hz for the samples of $Li_{6.4}La_3Zr_{1.7}W_{0.3}O_{12}$ based on the coupling model.

where β is the coupling parameter with a value between 0–1 that is an indicator of the degree of correlation or cooperativity in the relaxation process originating from the mutual interactions. Coupling parameter β decreases as the coupling strength increases. τ and τ^* are the coupled and decoupled relaxation time, respectively. The t_c was chosen as 10^{-12} s for metals and ionic conductor [31]. Based on the continuity of relaxation functions at $t = t_c$ and the Arrhenius law $\tau = \tau_0 exp(E/kT)$, we have

$$E^* = \beta E \tag{3}$$

$$\ln(\tau_0^*) = \beta \ln(\tau_0) + (1-\beta)\ln(t_c) \tag{4}$$

where E^* and E are the decoupled and coupled activation energies, τ_0^*

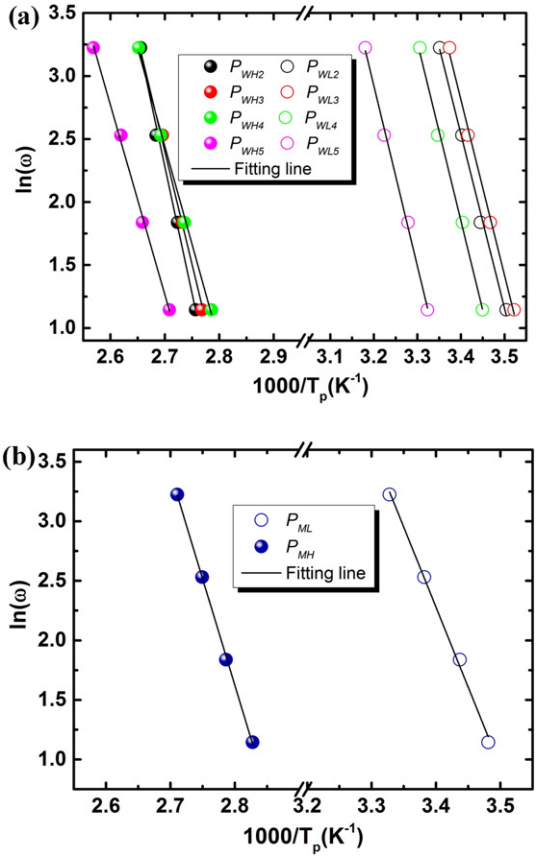

Fig. 11. Arrhenius plots of the two sub-peaks (P_L and P_H peaks) in (a) $Li_{7-2x}La_3Zr_{2-x}W_xO_{12}$ ($x = 0.2$–0.5) and (b) $Li_{6.4}La_3Zr_{1.7}Mo_{0.3}O_{12}$.

Table 2
Relaxation parameters of peak P_L and P_H in $Li_{7-2x}La_3Zr_{2-x}W_xO_{12}$ ($x = 0.2$–0.5) and $Li_{6.4}La_3Zr_{1.7}Mo_{0.3}O_{12}$ samples.

$Li_{7-x}La_3Zr_{2-x}M_xO_{12}$	M = W								M = Mo	
	$x = 0.2$		$x = 0.3$		$x = 0.4$		$x = 0.5$		$x = 0.3$	
	P_{L2}	P_{H2}	P_{L3}	P_{H3}	P_{L4}	P_{H4}	P_{L5}	P_{H5}	P_{L3}	P_{H3}
E (eV) (±0.07 eV)	1.19	1.74	1.20	1.57	1.22	1.35	1.23	1.28	1.16	1.54
τ_0 (s)	3.3×10^{-22}	2.3×10^{-25}	1.7×10^{-22}	8.5×10^{-23}	2.1×10^{-22}	5.0×10^{-20}	7.1×10^{-22}	6.4×10^{-19}	1.5×10^{-21}	3.8×10^{-23}
β	0.26	0.27	0.29	0.31	0.32	0.38	0.35	0.44	0.3	0.33
E^* (eV) (±0.02 eV)	0.31	0.47	0.35	0.49	0.39	0.51	0.43	0.56	0.35	0.51
τ_0^* (s)	3.4×10^{-15}	3.9×10^{-16}	1.5×10^{-15}	7.6×10^{-16}	8.0×10^{-16}	1.7×10^{-15}	6.0×10^{-16}	1.9×10^{-15}	2.2×10^{-15}	3.6×10^{-16}

and τ_0 are the pre-exponential factors of decoupled and coupled relaxation time, respectively.

By using the above coupling model combined by a nonlinear fitting method of the IF spectrum [19] the two prominent IF peaks observed in the $Li_{7-2x}La_3Zr_{2-x}M_xO_{12}$ (M = Mo and W) compounds can be well fitted by two IF peaks, as shown in Fig. 10, in which the fitting result of the IF peaks measured at 1 Hz for the $Li_{6.4}La_3Zr_{1.7}W_{0.3}O_{12}$ samples are particularly presented as the example. It can be seen from Fig. 10 that the relaxation strength of the low-temperature IF peak (labeled as peak P_L) are much higher than that of the high-temperature IF peak (labeled as peak P_L) in both W-substituted and Mo-substituted samples. As for the coupling parameter β, it is determined in the range of 0.26–0.44, which implies a relatively strong mutual interaction during lithium ion diffusion.

Through the nonlinear fitting of the IF curves, the peak temperature (T_P) of the two peaks under different measuring frequencies can be determined, and the corresponding coupled activation energy E and the pre-exponential factor τ_0 can thus be obtained in terms of the shift of peak temperature with measured frequency. In Fig. 11, the corresponding Arrhenius plots of the two relaxation peaks of $Li_{7-2x}La_3Zr_{2-x}M_xO_{12}$ (M = W, Mo) are presented, where the solid lines are the linear least-square fittings. The coupled relaxation parameters E and τ_0 can be deduced according to the Arrhenius relation, and the decouple relaxation parameters E^* and τ_0^* calculated based on the Eqs. (3) and (4) are listed in Table 2.

The fitting results indicate that the values of τ_0^* in the order of 10^{-16}–10^{-15} s falls in the range of typical values for processes of point defect relaxation, whatever for W or Mo substituting samples. Moreover, the decoupled activation energy of the high-temperature peak in the range of 0.47–0.56 eV is also in good agreement with the value of 0.45–0.49 eV for lithium ion diffusion obtained in conduction measurement. However for the low-temperature IF peak, the decoupled activation energy is in the range of 0.31–0.43 eV, which is lower than that of conduction measurement. It is the large difference between the activation energies of the two peaks that results in the large separation of the two IF peaks.

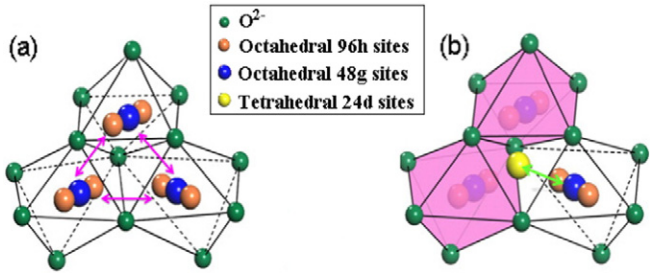

Fig. 12. Sketch map of the lithium environments in garnet-like structure L-L-M-O: (a) migration routes for lithium ions via 48 g (96 h)-48 g (96 h); (b) migration routes of lithium ions via 24d-48 g (96 h).

Different from the conductivity that is related to the average effect of long distance migration of carriers, the IF peaks reflect the short diffusion processes of lithium ions under periodic stress. It is suggested that the coexistence of two peaks in W and Mo substituted samples should have at least two different routes for lithium ion migration in the cubic $Li_{7-2x}La_3Zr_{2-x}M_xO_{12}$ (M = W, Mo) [11]. In the garnet-like cubic phase, the lithium ions distribute in a disordered state, and all Li sites with the same symmetry are only partially occupied with occupancies of about 88% at octahedral sites and 56% at tetrahedral sites, as experimentally predicted by neutron diffraction patterns [32]. Therefore there are plenty of intrinsic lithium vacancies to facilitate lithium ions migration in the cubic phase. The ab initio calculations further revealed that most of Li ions at the octahedral sites are actually deviated from their original central 48g sites and approach the 96h sites because of the Coulombic interaction [33]. Further considering the structural framework, the interstitial tetrahedral sites (24d) are surrounded by face-sharing octahedral sites, which actually exclude the possibility of direct diffusion among the neighboring tetrahedral sites. Therefore, the diffusion routes for lithium ions in cubic L–L–M–O systems have only two possibilities: 48g(96h)-48g(96h) and 48g(96h)-24d, as shown in Fig. 12(a) and (b), respectively. From the crystal structure of Li–La–M–O system, the diffusion distance between a tetrahedral 24d site and one of the nearest octahedral 48g(96h) sites is about 1.9898 Å, which is much shorter than the diffusion distance among the two neighboring 48g (or 96h) sites (2.5307 Å), and would correspond to a lower diffusion activation energy [34]. Hence for the IF peaks in $Li_{7-2x}La_3Zr_{2-x}M_xO_{12}$ (M = W, Mo), it can be suggested that the higher peak at lower temperature may be originated from the jump process among the nearest octahedral 48g(96h) sites and tetrahedral 24d sites i.e. 48g(96h)-24d, owing to its lower diffusion barrier, as shown in Fig. 12(b). Accordingly the lower peak at higher temperature may be originated from the jump process among the neighboring octahedral 48g(96h) sites, i.e. 48g(96h)-48g(96h), because of the higher diffusion barrier.

4. Conclusions

The effects of hexad substitution and the substituted concentration on lithium ion diffusion in $Li_{7-2x}La_3Zr_{2-x}M_xO_{12}$ (M = Cr, Mo, W) lithium conductors are investigated by AC impedance spectroscopy and internal friction (IF) techniques. The W substituted sample with $x = 0.2$ has a highest total conductivity of 8.7×10^{-5} S/cm, and the total conductibility of the $Li_{7-2x}La_3Zr_{2-x}W_xO_{12}$ ($x = 0.2$–0.5) decreases with the increasing W substituting concentration. Two prominent relaxation IF peaks were observed in the garnet-like $Li_{7-2x}La_3Zr_{2-x}M_xO_{12}$ (M = Mo, W) electrolytes, which was associated with the short distance diffusion of lithium ions or vacancies. The IF data were well analyzed using the coupling model. The relaxation strength of the IF peak decreases with the increasing W substituting concentration. The decrease of the relaxation strength of the IF peaks and total lithium ionic conductivity are all ascribed to the decreased lithium ions concentration n as well as the decreased mobility of the

lithium ions induced by the substitution of Zr^{4+} by W^{6+} and Mo^{6+}. The two IF peaks can be assumably ascribed to the two possible lithium ion diffusion routes via vacancies, i.e. 48g(96h)-24d for the low-temperature IF peak with a lower activation energy and 48g(96h)-48g(96h) for the high-temperature IF peak with a higher activation energy. The obtained experimental results also confirmed that different from the conductivity measurements, the IF method can be used as a sensitive and potential probe to explore the local diffusion process of carriers in detail in solid lithium electrolytes.

Acknowledgments

This work has been subsidized by the National Natural Science Foundation of China (Grant Nos. 51401203, 51301186, and 11274305), the Major Program of Development Foundation of Hefei Center for Physical Science and Technology (Grant No. 2014FXZY006) and the Shanxi Provincial Natural Science Foundation (No.15JK1833).

References

[1] K. Takada, Acta Mater. 61 (2013) 759–770.
[2] A. Aatiq, M. Me'ne'trier, L. Croguennec, E. Suard, C. Delmas, J. Mater. Chem. 12 (2002) 2971–2978.
[3] F. Mizuno, A. Hayashi, K. Tadanaga, M. Tatsumisago, Solid State Ionics 177 (2006) 2721–2725.
[4] U.V. Alpen, A. Rabenau, G.H. Talat, Appl. Phys. Lett. 30 (1977) 621–623.
[5] V. Thangadurai, W. Weppner, Adv. Funct. Mater. 15 (2005) 107–112.
[6] Y.X. Gao, X.P. Wang, W.G. Wang, Z. Zhuang, D.M. Zhang, Q.F. Fang, Solid State Ionics 181 (2010) 1415–1419.
[7] S. Ohta, T. Kobayashi, T. Asaoka, J. Power, Sources 196 (2011) 3342–3345.
[8] S.W. Baek, J.M. Lee, T.Y. Kim, M.S. Song, Y. Park, J. Power Sources 249 (2014) 197–206.
[9] Y. Jin, P.J. McGinn, J. Power, Sources 196 (2011) 8683–8687.
[10] Y.H. Zhang, F. Chen, R. Tu, Q. Shen, L.M. Zhang, J. Power, Sources 268 (2014) 960–964.
[11] X.P. Wang, Y.X. Gao, Y.P. Xia, Z. Zhuang, T. Zhang, Q.F. Fang, Phys. Chem. Chem. Phys. 16 (2014) 7006–7014.
[12] J. Awaka, A. Takashima, K. Kataoka, N. Kijima, Y. Idemoto, J. Akimoto, Chem. Lett. 40 (2011) 60–62.
[13] H. Buschmann, J. Dolle, S. Berendts, A. Kuhn, P. Bottke, M. Wilkening, P. Heitjans, A. Senyshyn, H. Ehrenberg, A. Lotnyk, V. Duppel, L. Kienlee, J. Janek, Phys. Chem. Chem. Phys. 13 (2011) 19378–19392.
[14] R. Djenadic, M. Botros, C. Benel, O. Clemens, S. Indris, A. Choudhary, T. Bergfeldt, H. Hah, Solid State Ionics 263 (2014) 49–56.
[15] R. Murugan, S. Ramakumar, N. Janani, Electrochem. Commun. 13 (2011) 1373–1375.
[16] K. Liu, C.A. Wang, Electrochem. Commun. 48 (2014) 147–150.
[17] M. Kotobuki, K. Kanamura, Y. Sato, T. Yoshida, J. Power, Sources 196 (2011) 7750–7754.
[18] X.P. Wang, Q.F. Fang, Phys. Rev. B 65 (2002) 064304–064309.
[19] Y.X. Gao, Z. Zhuang, H. Lu, X.P. Wang, Q.F. Fang, Solid State Phenom. 184 (2012) 116–121.
[20] X.P. Wang, W.G. Wang, Y.X. Gao, T. Zhang, Q.F. Fang, Mater. Sci. Eng. A 521 (2009) 87–89.
[21] X.P. Wang, Y. Xia, J. Hu, Y.P. Xia, Z. Zhuang, L.J. Guo, H. Lu, T. Zhang, Q.F. Fang, Solid State Ionics 253 (2013) 137–142.
[22] J. Rodrguez-Carvajal, Physica B 192 (1993) 55–69.
[23] L. Dhivya, N. Janani, B. Palanivel, R. Murugan, AIP Adv. 3 (2013) 082115.
[24] R.D. Shannon, Acta Cryst 32 (1976) 751–767.
[25] Y.X. Gao, X.P. Wang, W.G. Wang, Q.F. Fang, Solid State Ionics 181 (2010) 33–36.
[26] Y.T. Li, J.T. Han, C.A. Wang, S.C. Vogel, H. Xie, M.W. Xu, J.B. Goodenough, J. Power, Sources 209 (2012) 278–281.
[27] M.M. Ahmad, M.M. Al-Quaimi, Phys. Chem. Chem. Phys. 17 (2015) 16007–16014.
[28] A.S. Nowick, B.S. Berry, Anelastic Relaxation in Crystalline Solids, Academic Press, New York and London, 1972.
[29] K.L. Ngai, Disorder Effects on Relaxation Processes, Springer-Verlag, Heidelberg, 1994.
[30] K.L. Ngai, Y.N. Wang, L.B. Magalas, J. Alloys Compd. 327 (1994) 211–212.
[31] K.L. Ngai, H.H. Jain, Solid State Ionics 362 (1986) 18–19.
[32] H. Xie, J.A. Alonso, Y.T. Li, M.T. Ferna'ndez-D'az, J.B. Goodenough, Chem. Mater. 23 (2011) 3587–3589.
[33] M. Xu, M.S. Park, J.M. Lee, T.Y. Kim, Y.S. Park, E. Ma, Phys. Rev. B: Condens. Matter Mater. Phys. 85 (2012) 052301.
[34] R. Jalem, Y. Yamamoto, H. Shiiba, M. Nakayama, H. Munakata, T. Kasuga, K. Kanamura, Chem. Mater. 25 (2013) 425–430.